

## Managing understory light to maintain a mixture of species with different shade tolerance



Gauthier Ligot<sup>a,\*</sup>, Philippe Balandier<sup>d</sup>, Benoît Courbaud<sup>c</sup>, Mathieu Jonard<sup>b</sup>, Daniel Kneeshaw<sup>e</sup>, Hugues Claessens<sup>a</sup>

<sup>a</sup> Univ. de Liège, Gembloux Agro-Bio Tech, Unité de Gestion des Ressources forestières et des Milieux naturels, 2, Passage des Déportés, B-5030 Gembloux, Belgium

<sup>b</sup> UCL, Louvain-la-Neuve, Earth & Life Institute, Croix du Sud, 2 bte L7.05.05, B-1348 Louvain-la-Neuve, Belgium

<sup>c</sup> Irstea, Mountain Ecosystems Research Unit, 2 rue de la Papeterie, 38402 Saint Martin d'Hères, France

<sup>d</sup> Irstea, U.R. Ecosystèmes Forestiers (EFNO), Domaine des Barres, 45290 Nogent-sur-Vernisson, France

<sup>e</sup> Centre d'Étude de la Forêt, Case postale 8888, succursale Centre-ville, Montreal, QC H3C 3P8, Canada

### ARTICLE INFO

#### Article history:

Received 18 February 2014

Received in revised form 5 May 2014

Accepted 6 May 2014

#### Keywords:

Cutting simulation

Continuous-cover forestry

Oak

European beech

Light

### ABSTRACT

Close-to-nature management of forests has been increasingly advocated. However forest managers often face difficulties in maintaining mixtures of species with different shade tolerance. In uneven aged stand management, understory light can be manipulated by modifying stand structure and composition, in addition to stand density. Using a forest radiative transfer model, we analyzed how different cutting strategies could modify light availability under the post-harvest canopy. To calibrate the model, we measured and mapped trees in 27 plots with structures ranging from secondary-successional oak forests to late-successional beech forests. We measured understory light and crown openness and verified that our forest radiative transfer model well captured the variability of understory light among the studied stands ( $R^2 = 87\%$ ). We then compared cutting strategies varying in type and intensity and provided indications to promote the regeneration of mixtures of species of different shade tolerances. In particular, creating gaps of about 500 m<sup>2</sup> provided adequate light for small regeneration clumps. Cutting from below, species-specific cutting and uniform cutting were also appropriate for tree regeneration but uniform cutting required higher harvest intensity. Cutting from above slightly increased understory light and promoted more shade tolerant species.

© 2014 Elsevier B.V. All rights reserved.

### 1. Introduction

Close-to-nature management of forests has been increasingly advocated and practiced. Foresters attempt to mimic natural processes in order to produce wood and to preserve ecosystem services and diversity (Schütz, 1999). This concept is generally practiced using continuous-cover forestry systems, relying on natural regeneration, maintaining irregular stand structure and a mixture of tree species (Pommerening and Murphy, 2004; Bruciamacchie and de Turckheim, 2005; Schütz et al., 2012). The major difficulty with this system is in controlling the composition and the growth of the natural regeneration, especially of the regeneration of less shade-tolerant species.

Naturally, when they are abundant in the overstory or understory, shade-tolerant species suppress the regeneration of less shade-tolerant species in continuous-cover forestry system

because canopy openings are usually limited. As a case in point, beech (*Fagus*) is a common genus in the northern hemisphere whose species are known to be very shade-tolerant and to suppress less shade-tolerant species in the absence of severe perturbation (Kunstler et al., 2005; Beaudet et al., 2007; Wagner et al., 2010; Takahashi and Goto, 2012; Ligot et al., 2013). Beech juveniles survive and invade the understory even under a closed canopy. After even a slight canopy release, that lets in 10% of above canopy light, beech juveniles thrive whereas most other species cannot survive for long (Emborg, 1998; Stancioiu and O'Hara, 2006). In understories with more than 20% of above canopy light, such as after moderate canopy release, less shade-tolerant species grow well. Nevertheless, in these conditions, beech juveniles grow faster (Kunstler et al., 2005; Beaudet et al., 2007; Takahashi and Goto, 2012; Ligot et al., 2013) and are often taller than the companion species.

Controlling understory light is therefore a key factor to regenerate mixed stands (Lieffers et al., 1999). The control of understory light with partial cuttings requires properly modifying stand

\* Corresponding author. Tel.: +32 81622320; fax: +32 81622301.

E-mail address: [gligot@ulg.ac.be](mailto:gligot@ulg.ac.be) (G. Ligot).

structure and composition in addition to solely managing stand density. To date, this question of how changes in stand structure and composition affects understory light has rarely been addressed, especially for heterogeneous broadleaved forests. Only a few field experiments successfully defined levels of canopy openness suitable for the regeneration of mixed species (von Lüpke, 1998; Prévost and Pothier, 2003) while simulation studies have been limited to particular ecosystems. Cutting groups of spatially aggregated trees or creating gaps has been reported to drastically increase light availability for the regeneration in boreal mixed-woods (Coates et al., 2003; Beaudet et al., 2011), even-aged western hemlock or douglas-fir forests (Sprugel et al., 2009) or uneven-aged spruce forests (Courbaud et al., 2001; Lafond et al., 2013). Additionally, cutting understory poles and trees with branches immediately above the regeneration, or cutting from below in some way, has often been recommended for shelterwood systems as these poles and trees, unless removed, compete strongly with regeneration for nutrients, water and light resources (Nyland, 1996). Moreover, we suppose that removing shade-tolerant species increases understory light more than removing trees randomly because shade-tolerant species usually have wider, deeper and denser crowns than less shade-tolerant species (Coates et al., 2003; Beaudet et al., 2011).

We therefore attempted to explore how silvicultural regeneration treatments modifying stand structure and composition affect understory light in order to identify the best treatment to promote the regeneration of mixed species. In particular, we aimed to:

1. compare different cutting scenarios hypothesizing that, at similar levels of harvest intensity, gap creation, cutting from below, removing shade-tolerant species (species-specific cutting), cutting randomly and cutting from above induced respectively a high to low responses in transmitted light ( $H_1$ );
2. test whether our first hypothesis is general or depends on initial stand structure ( $H_2$ );
3. identify the combinations of cutting scenarios that maximize the understory area receiving 10–20% (levels favorable to regeneration of shade-tolerant species such as beech regeneration) or 20–40% (levels favorable to regeneration of mid-tolerant species) and above 40% (little light limitations for most regeneration) of above canopy light.

## 2. Methods

### 2.1. Study area

We studied light management as a regeneration treatment for acidophile medio-European beech forests (CORINE classification 41.111) mainly composed of European beech (*Fagus sylvatica* L.) and sessile oak (*Quercus petraea* (Matt.) Lieb). These forests have been managed with continuous-cover forestry systems for several decades and it has been noticed that the proportion of less shade-tolerant companion species has decreased (von Lüpke, 1998; Alderweireld et al., 2010). This underlines the failure of current practices to promote the coexistence of species mixtures. Yet, sustaining oak in beech forests, as well as maintaining mixtures of tree species in general, is important for biodiversity, forest resiliency, soil fertility, recreational and timber production issues.

The study area was located in the Belgian Ardennes (50°15'N, 5°40'E). Dominant soils are well drained brown acidic soils (WRB soil classification) of variable depth that developed on hercynian oligotrophic schist and sandstone substrates. Precipitation ranges from 930 to 1200 mm year<sup>-1</sup> and the mean annual temperature is about 9 °C.

We selected 27 sites with varying stand structures and compositions and with established regeneration of oak and (or)

beech. These studied stands characterized the diversity of forest structures that can be found during forest succession of early-successional oak forests to late-successional pure beech forests (Fig. 1). All of the studied stands are in public forests. With the gradual degradation of the market of small oak timber during the 20th century, they have been managed with continuous-cover forestry systems in order to progressively convert oak coppices or oak coppices with standards to high forests. Forest managers have usually maintained high forest stocking of adult trees promoting beech regeneration. Nevertheless, during the last decade, beech decay (Henin et al., 2003) has opened the canopy of some of these forests providing opportunities for the regeneration of less shade-tolerant species.

Every tree with a circumference greater than 40 cm was mapped and measured. We measured the circumference at breast height, total height ( $H$ ), and height to the base of the crown for each tree. On 13 sites, we also measured at least 4 crown radii for every tree. Besides oak and beech, our data set contained 7% hornbeam (*Carpinus betulus* L.), 4% small coniferous trees (*Pseudotsuga menziessi* (Mirb.) Franco, *Picea abies* (L.) Karst, and *Pinus sylvestris* L.), 2% birches (*Betula pendula* Erth, *Betula pubescens* Erth), and 2% other broadleaved species (*Acer pseudoplatanus* L., *Acer platanoides* L., *Sorbus aucuparia* L., and *Corylus avellana* L.).

The inventoried plots had an oval shape of variable area because they surrounded fenced areas in which advanced regeneration has been studied for a companion study (Ligot et al., 2013). Trees were measured if they were located at a distance of less than 20 m from the fence. Plot area ranged from 2070 m<sup>2</sup> to 10,540 m<sup>2</sup> with an average of 4340 m<sup>2</sup>.

### 2.2. Model development and implementation

The forest radiative model named SamsaraLight was implemented in the forest simulation platform Capsis (Dufour-Kowalski et al., 2012). Courbaud et al. (2003) described a first version of this radiative model and validated it for an irregular Norway spruce stand (*Picea abies* (L.) Karst). Since 2003, the model has been improved and now enables users to model crowns with asymmetric ellipsoids (Appendix A).

We set SamsaraLight to sample 130 diffuse and 81 direct ray directions for each month of the growing period (from April to October). Ray directions are sampled at regular increasing zenithal angles with a starting value of 10° and an angle step of 15°. For every direction, parallel rays are cast at ground level in either cell centers or any other specified locations (virtual sensor). SamsaraLight then identifies the interceptions of light rays by tree crowns and computes radiation attenuation using Beer's law (Eq. (1)).

SamsaraLight predicts transmitted light within a rectangular plot. Since our inventory plots were not rectangular, we developed an algorithm that added virtual trees in order to obtain a rectangular plot (Fig. 2). For each site, virtual trees were randomly drawn with replacement from the measured trees. Their location outside the inventoried area was then randomly generated. This process was repeated until the basal area of the rectangular plot equaled the basal area of the inventoried plot. The number of virtual trees created in each plot ranged between 0 and 68, and the area over which they were simulated represented on average 28% of the rectangular plot area.

### 2.3. Model parameterization

SamsaraLight required defining the dimensions and leaf area density of the modeled crowns. We adjusted allometric relationships using the nonlinear least squares method (R Core Team, 2013) in order to estimate missing crown radii for the six main groups of species: beech, oak, hornbeam and birches, other

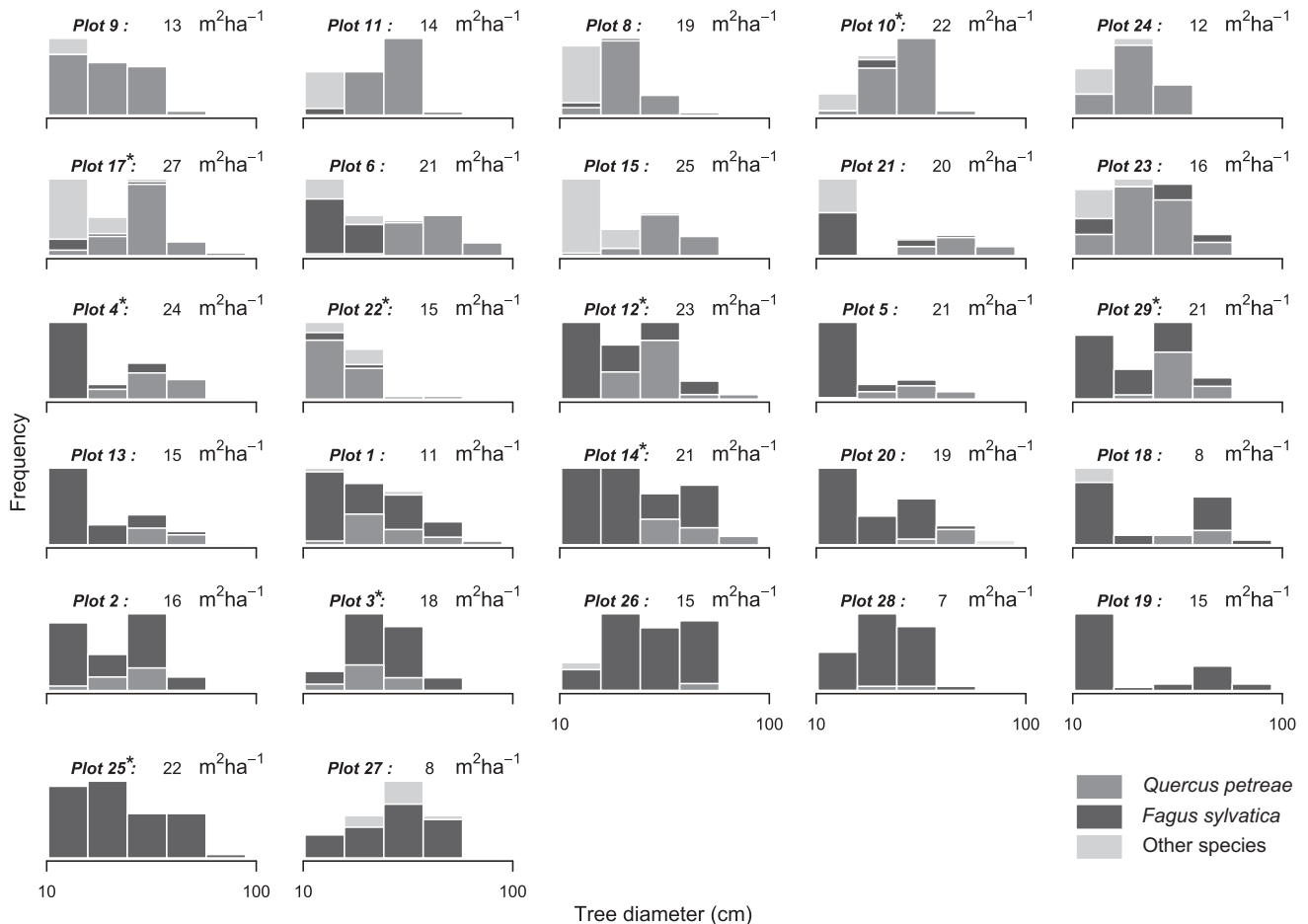


**Fig. 1.** Stand structure and composition of the 27 studied plots expressed as tree frequency by diameter class. The charts are sorted by decreasing proportion of oak. Plot basal area is reported next to the plot id number showing no trend between plot basal area and plot composition. The asterisks next to plot id number denote the 9 plots where initial mean percentage of above canopy light (PACL) was below 20%.

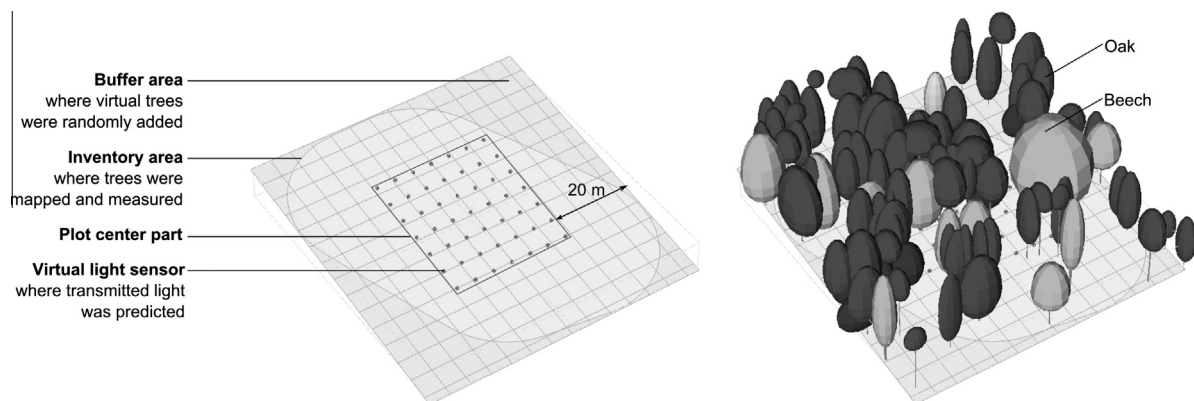


**Fig. 2.** Three dimensional visualizations of the different zones within a plot (plot ID 22) with and without trees. In order to evaluate the cutting scenarios, our model was set to predict the percentage of above canopy light at 2 m above forest ground (virtual light sensor) and at every intersection of a 7 m × 7 m grid within the center part of the plots.

broadleaved species, and coniferous species. Crown radii were best modeled with power functions of tree diameter (dbh) similarly to Beaudet et al. (2011). Crown leaf area density (LAD) was estimated with photographs of isolated crowns similarly to the method used to estimate crown openness (Canham et al., 1999; Beaudet and Messier, 2002; Astrup and Larson, 2006). This method is rapidly executed in comparison to previously reported methods using leaf samples or leaf traps (Bartelink, 1997; Jonard et al., 2006) or vertical line intersect sampling methods (Nock et al., 2008) but it

applies only to trees with relatively isolated crowns. We took 112 photographs of isolated crowns of 21 oaks, 13 beeches, 8 birches and 4 hornbeams. The photographs were processed with PiafPhotem (Adam et al., 2006) in order to compute the gap fraction,  $p$ . Additionally, for every photographed crown, we recorded 4 crown radii, crown base height and tree height. We computed the path length,  $l$ , as the distance between the intersections between the modeled crown ellipsoids (Appendices A–D) and the photograph direction. Photograph direction was computed from

the recorded photograph elevation angle and the estimated distance to the trunk (Appendix B). The inversion of Beer's law (Eq. (1)), with the common assumption of spherical distribution of leaves ( $k = 0.5$ ), was used to estimate LAD (Phattaralerphong et al., 2006; Da Silva et al., 2012). We could have used  $k$ -LAD instead of LAD. Although this would allow us to not fix  $k$ , it would not have allowed us to compare LAD values with other published works.

$$p \approx \frac{I}{I_0} = \exp(-k \cdot l \cdot \text{LAD}) \quad (1)$$

with  $I$  and  $I_0$  the transmitted irradiance and the incident irradiance, respectively.

We finally modeled the LAD estimates for beech and oak. We obtained the best fits with a polynomial function of dbh adjusted with the linear least squares method (R Core Team, 2013). For the other species we did not collect enough data to model LAD as a function of dbh. Nevertheless, Courbaud et al. (2003) mentioned that SamsaraLight sensitivity to leaf area density was low between 0.3 and 0.9  $\text{m}^2 \text{m}^{-3}$ . We assumed LAD to be 0.6  $\text{m}^2 \text{m}^{-3}$  for all other species as 0.6 corresponded to the average of all measured trees. Trunks were modeled as cylinders of dbh diameter and crown base height. Trunk do not transmit light.

SamsaraLight additionally required monthly meteorological records of total and diffuse irradiances in  $\text{MJ m}^{-2}$ . We computed such monthly averaged data from data recorded between 2007 and 2011 by the meteorological institute of Belgium in Humain (50°33'N 5°43'E). Furthermore, we set SamsaraLight to predict percentages of above canopy light (PACL) at 2 m above the forest floor at each intersection of a  $7 \times 7$  rectangular grid (Fig. 2). We thus obtained 49 estimates of PACL for each simulation.

#### 2.4. Model evaluation

In mid-July 2010, we took 307 hemispherical photographs in 19 sites. The photographs were taken just before sunrise and above the regeneration of the plots that were installed every 4 m following a square grid (Ligot et al., 2013). The number of photographs per site depended therefore on the area of each site and ranged between 6 and 39. We then computed the percentage of above canopy light ( $\text{PACL}_{\text{photo}}$ ) that is transmitted through the canopy between April 1st and October 31st 2012. For the sole purpose of model evaluation, we additionally measured and mapped every stem greater than 20 cm circumference in circular plots of 15 m radius and every stem greater than 7.5 cm circumference in circular plots of 7 m radius. These concentric plots were centered around the points where hemispherical photographs were taken. We compared the hemispherical photograph light estimates with SamsaraLight predictions ( $\text{PACL}_{\text{model}}$ ) computed for the same period and at the same locations (i.e. not at the intersection points of the grid used for the evaluation of the cutting scenarios).

In order to evaluate model predictions, we adjusted linear models with the ordinary least square method between  $\text{PACL}_{\text{model}}$  and  $\text{PACL}_{\text{photo}}$ . Next, we computed the confidence intervals ( $\alpha = 0.05$ ) of model coefficients in order to appreciate the deviation of the modeled relationship with a 1:1 relationship. Similarly to Da Silva et al. (2012), we also compared the cumulative distribution function (CDF) of  $\text{PACL}_{\text{photo}}$  and  $\text{PACL}_{\text{model}}$  for every site. We computed a Kolmogorov–Smirnov test (K–S test) to quantify and test the distance between the two CDFs. The null hypothesis being that the samples are drawn from the same population.

#### 2.5. Cutting scenarios

For the 27 inventoried stands, we simulated 5 cutting types that reproduced 5 silvicultural regeneration strategies commonly

practiced in forests of the Belgian Ardennes; namely: cutting from above, cutting from below, gap creation, species-specific cutting and uniform cutting (Table 1). Cutting from above harvests the most valuable trees. Typically, the trees with a diameter greater than the exploitable diameter are cut i.e. these are diameter limit cuts. In contrast, cutting from below harvests small trees with low economic value. Such a strategy is typically applied to promote the growth of dominant trees, increase light for natural regeneration and mimics self-thinning. Cutting that creates gaps are especially used to increase light for a clump of saplings and promote regeneration. Species-specific cutting has been practiced recently because oak has become scarce. Therefore, foresters conserve oak seed trees even if, for example, their diameter exceeds the exploitable diameter or if they are wounded. Finally, we simulated uniform cuttings in which trees were randomly harvested. This scenario can be considered to be the control treatment.

The 5 algorithms of the 5 cutting types started computing  $\text{score}_t$  (Table 1) for every tree and then cut the trees by order of decreasing  $\text{score}_t$  until the harvest intensity level was reached.  $\text{score}_t$  computed for cuttings from below and from above were on average greater for narrow and large trees, respectively.  $\text{score}_t$  included a random component that ensured that tree selection differed between simulations. The weight given to this random contribution was set to 0.2 so that the distribution of the diameter of cut trees followed a realistic normal distribution. Gap creation scenarios harvested trees around a random location that must lie within the central part of the plots (Fig. 2). Furthermore with cutting intensities greater or equal to 0.4, the gap radius was often greater than 20 m which corresponded to the buffer distance between the plot boundary and the center part of the plots (Fig. 2). In such cases, the gap shape became a truncated circle. These algorithms are now available in Capsis for most individual tree growth models.

The 5 cutting types were applied to the 27 stands with 4 different levels of harvest intensity (10%, 20%, 40% and 60% of initial plot basal area). Since the algorithms of every cutting type had stochastic components, we repeated the simulation 10 times. For each simulation, 49 estimates of PACL were computed according to the grid introduced in Section 2.3. We therefore tested 20 cutting scenarios with 5427 simulations and 265,923 computations of  $\text{PACL}_{\text{model}}$ .

#### 2.6. Statistical analyses of cutting scenarios

In order to compare the different scenarios, we computed the differences between the average of the 49 estimates of transmitted light before and after harvesting ( $\Delta\text{PACL}$ ). Then, we adjusted a linear mixed model with lme4 R package (Bates et al., 2013) in order to quantify the relationship between  $\Delta\text{PACL}$  and cutting intensity ( $I_i$ ).

$$\begin{aligned} \Delta\text{PACL}_{ijkl} &= (b_i + \beta_{ji})I_i + \varepsilon_{ijkl} \\ \beta_{ji} &\sim N(0, \theta_\beta) \\ \varepsilon_{ijkl} &\sim N(0, \theta_\varepsilon) \end{aligned} \quad (2)$$

With  $i, j, k, l$  the indices corresponding to the cutting intensity, plot, the simulation run and the cutting type, respectively.  $b_i$  was the fixed-effect parameter which was estimated for each “ $I$ ” cutting type.  $\beta_{ji}$  was a random-effect parameter varying between plot and cutting type. Similarly to the residual term,  $\beta_{ji}$  followed a centered normal distribution. This model assumed that  $\Delta\text{PACL}$  was proportional to  $I_i$  and that the slope of this relationship ( $b_i$ ) varied with cutting type and initial site conditions. The hypothesis  $H_1$  was tested computing the approximate confidence intervals of  $b_i$ . These confidence intervals were obtained from the likelihood profile of  $b_i$  (Bates et al., 2013).

In order to further analyze how initial stand structure affected the response ( $H_2$ ), we fitted five additional models that included

**Table 1**

Description of the 5 cutting types. With  $(x_t; y_t)$  the tree coordinates,  $(x_g; y_g)$  the random gap center coordinates that must be within the central part of the plot (i.e. within  $(x_{\min}, x_{\max}, y_{\min}, y_{\max})$ ,  $dbh_t$  the diameter of tree  $t$ ,  $dbh_{\min}$  and  $dbh_{\max}$  the minimum and maximum of  $dbh$ ,  $u$  a random number generated between 0 and 1.

Cutting type	Description	Score <sub>t</sub>
Uniform cutting	Random harvest of trees	$score_t \sim u$
Species-specific cutting	Preferential harvest of beech and hornbeam ( $\beta = 2$ ), then the other species ( $\beta = 1$ ) and finally oak ( $\beta = 0$ )	$Score_t = \beta + u$
Cutting from below	Preferential harvest of small trees	$score_t = 0.2u + 0.8 \left(1 - \frac{dbh_t - dbh_{\min}}{dbh_{\max} - dbh_{\min} + 1}\right)$
Cutting from above	Preferential harvest of large trees	$score_t = 0.2u + 0.8 \left(1 - \frac{dbh_{\max} - dbh_t}{dbh_{\max} - dbh_{\min} + 1}\right)$
Gap creation	Harvest of all trees around a gap center. The location of the gap center was determined at random but must be within the central part of a plot (Fig. 2).	$score_t = -\sqrt{(x_t - x_g)^2 + (y_t - y_g)^2}$ $x_g \sim U_{[x_{\min}, x_{\max}]}$ $y_g \sim U_{[y_{\min}, y_{\max}]}$

the effects of 5 different stand structure parameters (denoted by  $P$  in Eq. (3)). These parameters were stand basal area (BA), quadratic mean diameter (dg), basal area proportion of oak ( $P_{\text{oak}}$ ), standard deviation of dbh ( $\theta_{\text{dbh}}$ ), Clark–Evans aggregation index (CE) and basal area of trees with dbh smaller than 25 cm (BAS). With the exception of BAS, they have commonly been used to describe stand density and structure in similar studies (Sprugel et al., 2009; Beaudet et al., 2011; Lafond et al., 2013). These indices describe the stand density and structure before harvest. The Clark–Evans aggregation index (Eq. (4)) gives values greater than 1 for regular tree distributions and lower than 1 for aggregated tree distributions. The basal area of small trees (BAS) was added because poles and small trees were sometimes abundant in the understory and was expected to capture a high proportion of transmitted radiation. We tested the addition of the corresponding fixed-effect parameter  $c_5$  with the log likelihood ratio test (Bates et al., 2013).

$$\Delta\text{PACL}_{ijkl} = (b_i + c_i \cdot P_j + \beta_{ji})I_i + \varepsilon_{ijkl} \quad (3)$$

$$\text{CE} = \frac{\bar{r}}{0.5\sqrt{A/N}} \quad (4)$$

where  $c_i$  is an additional fixed-effects parameter varying with cutting type, the mean distance between trees and their nearest neighbor,  $A$  is the plot area and  $N$  is the number of trees within the plot. Next, we computed the slope of this relationship ( $b_i + c_i \cdot P_j$ ) for the different cutting types and for the observed ranges of the parameters. We could thus determine whether our first hypothesis was verified for all of the initial stand conditions.

Next, we created four classes of PACL. These classes had PACL values ranging between 0–10%, 10–20%, 20–40%, and 40–100%. They corresponded respectively to light levels that are unfavorable to natural regeneration of tree species, favorable to beech sapling growth, favorable to beech and oak sapling growth and above light saturation point (Ligot et al., 2013).

Furthermore, we computed the average frequency of the predictions by PACL classes and cutting intensity. In order to provide a guide to forest managers, we repeated these computations replacing the harvest intensity by the resulting post-harvest basal area. We restricted these analyses to the 9 plots where the mean PACL before cutting was less than 20%, i.e. where cutting was necessary to promote the natural regeneration of less shade-tolerant species.

### 3. Results

#### 3.1. Tree inventory

According to the field data, stand composition and stand density varied considerably between study sites (Fig. 1 and Table A1 in Appendix). The proportion of oak in the overstory ranged

between 0% and 98%. High proportions of oak occurred mostly in stands with high basal area ( $r = 0.389$ ,  $P = 0.045$ ) and low quadratic mean diameter ( $r = -0.523$ ,  $P = 0.004$ ). Additionally, in some sites, the distribution of tree diameters followed an inverted j-shaped curve while in other sites it approximated a bell-shaped curve (Fig. 1). Tree aggregation was greater in stands with complex vertical structure. Clark–Evans aggregation index was indeed negatively correlated with the standard deviation of tree diameter ( $r = -0.500$ ,  $P = 0.008$ ).

#### 3.2. Allometric relationships

The power function models of crown radius fitted well the 6 groups of species with root mean square error lower than 81 cm (Table 2). For comparable tree dbh, hornbeam and beech trees had wider crowns than oak trees.

Estimates of crown leaf area density (LAD, in  $\text{m}^2 \text{m}^{-3}$ ) varied noticeably from tree to tree and even from photography to photography of the same tree. Foliage biomass is usually assumed to depend on sapwood area (pipe model) (Shinozaki et al., 1964) and hence also to tree dbh. However, tree dbh explained only 48% and 30% of LAD variability for oak and beech trees, respectively (Table 3). LAD decreased with tree dbh and more so for beech than for oak. Additionally, LAD stopped decreasing for beech at around 50 cm dbh and then started to increase gently. Our LAD estimates matched previously reported values of leaf area for beech and oak (Bartelink, 1997; Jonard et al., 2006) and were in the range of reported LAD values for broadleaved species (Stadt and Lieffers, 2000; Piboule, 2001; Gersonde et al., 2004; Sprugel et al., 2009).

#### 3.3. Light model evaluation

There was a good linear relationship between the modeled  $\text{PACL}_{\text{model}}$  and the measured  $\text{PACL}_{\text{photo}}$  ( $R^2 = 68\%$ , Fig. 3a) although our model tended to overestimate  $\text{PACL}_{\text{photo}}$  (intercept significantly greater than 0 and the slope not significantly different from 1). The model predicted better PACL values when averaged at the site level ( $R^2 = 87\%$  with intercept not significantly different from 0 and the slope slightly significantly greater than 1, Fig. 3b).

According to the K–S test statistic, the distributions of  $\text{PACL}_{\text{model}}$  and  $\text{PACL}_{\text{photo}}$  differed significantly ( $P < 0.05$ ) from each other for 7 of the 19 plots (see K–S test statistic of Fig. 4). Nevertheless, the differences were noteworthy for only 5 plots in which  $\text{PACL}_{\text{model}}$  clearly overestimated  $\text{PACL}_{\text{photo}}$ . These plots were characterized by an abundance of small beech and hornbeam trees that covered the regeneration layer where  $\text{PACL}_{\text{photo}}$  measures were taken. But even in these cases, the variation between the distributions  $\text{PACL}_{\text{model}}$  and  $\text{PACL}_{\text{photo}}$  was less than 15%. Moreover, model performance appeared independent of stand composition as highlighted by Fig. 4 in which plots were ordered by decreasing oak proportion.

**Table 2**  
Parameter estimates and their 95% confidence intervals with  $\alpha = 0.05$  (CI) for the power function model between crown radius (CR) and tree diameter (dbh):  $CR = a \cdot (dbh)^b$ . Also presented are the number of measured trees ( $n$ ), the ranges of measured dbh, the ranges of measured CR and the root mean square error (RMSE).

Species	$n$	dbh (cm)	CR (m)	$a$		$b$		RMSE (m)
				Estimate	CI	Estimate	CI	
Oak	314	2.4;92.3	0.5;7.7	0.310	0.240;0.396	0.698	0.634;0.764	0.808
Beech	475	2.4;80.5	0.3;10.4	0.742	0.679;0.808	0.516	0.492;0.541	0.755
Hornbeam	67	2.4;42.0	0.8;5.1	0.854	0.682;1.054	0.503	0.425;0.583	0.632
Birch	40	2.4;49.7	0.6;3.8	0.536	0.457;0.621	0.493	0.444;0.545	0.266
Other hardwoods	43	2.5;19.8	0.7;3.4	0.960	0.616;1.436	0.325	0.144;0.515	0.576
Other conifers	45	2.4;21.0	0.6;2.5	0.516	0.441;0.601	0.509	0.440;0.579	0.179

**Table 3**  
Parameter estimates and their 95% confidence intervals with  $\alpha = 0.05$  (CI) for the polynomial model between crown leaf area density (LAD) and tree diameter (dbh):  $LAD = a + b \cdot dbh + c \cdot dbh^2$ . Also presented are tree number ( $n_t$ ), photograph number ( $n_p$ ), ranges of measured dbh (in cm), ranges of estimated LAD (in  $m^2 m^{-3}$ ) and the root mean square error (RMSE). We assumed LAD to be  $0.6 m^2 m^{-3}$  for all other species.

Species	$n_t$	$n_p$	dbh (cm)	LAD ( $m^2 m^{-3}$ )	$a$		$b$		$c$		RMSE ( $m^2 m^{-3}$ )
					Estimate	CI	Estimate	CI	Estimate	CI	
Beech	13	71	7.6–72.3	0.2–2.4	1.720	1.450;1.990	−0.059	−0.076;−0.042	6.19E−4	4.15E−4;8.22E−4	0.320
Oak	21	112	5.4–71.9	0.2–2.3	1.207	0.972;1.441	−0.033	−0.046;−0.019	3.05E−4	1.32E−4;4.79E−4	0.288
Hornbeam	4	23	19.7–32.8	0.3–0.8	0.522	0.469;0.575					0.120
Birch	8	42	12.7–34.4	0.4–0.9	0.595	0.562;0.629					0.106

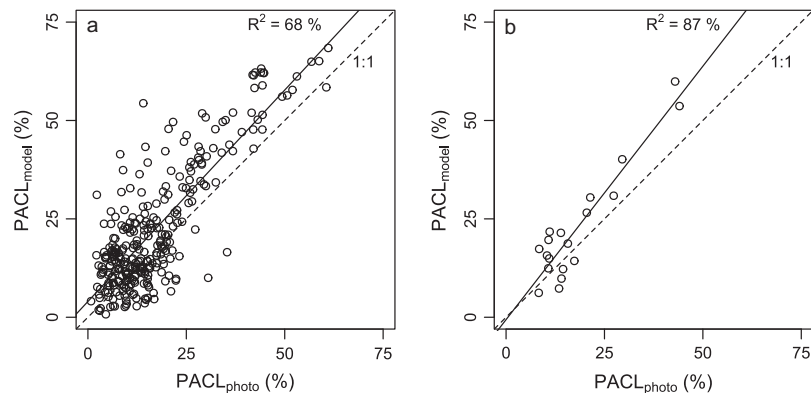


**Fig. 3.** Relationships between predicted percentages of above canopy light ( $PACL_{model}$ ) and the percentages of above canopy light estimated from hemispherical photographs ( $PACL_{photo}$ ): point-to-point comparison of all  $PACL_{model}$  and  $PACL_{photo}$  (a) and comparison of the  $PACL_{model}$  and  $PACL_{photo}$  averaged by site. The dotted lines show the 1:1 relationships, whereas the full lines correspond to the linear least squares regressions.

### 3.4. Cutting scenarios

The different cutting scenarios harvested the same quantities of basal area but caused very different modifications to stand structure.

Firstly, post-harvest density varied notably between cutting scenarios. Cutting from below harvested the greatest number of trees while cutting from above harvested the fewest number of trees. The other cutting scenarios harvested an intermediate number of trees.

Secondly, harvests affected stand composition. Species-specific cutting increased the proportion of oak trees. Moreover, because the understory was mainly composed of shade-tolerant species (beech and hornbeam), cutting from below also tended to increase the proportion of oak trees. Cutting from above tended to harvest more oak trees than the other scenarios.

Thirdly, stand spatial structure was little affected by harvests except by gap creation. Gap creation increased the aggregation of trees as indicated by a reduction in the Clark–Evan aggregation index. Even at low harvest intensity, large gaps were created and remaining trees were aggregated along gap periphery. For

example, removal of 10% and 20% stand basal area using gap harvesting led to an average opening of  $475 m^2$  and  $1182 m^2$ , respectively.

### 3.5. Simulation results

The increase in understory light levels ( $\Delta PACL$ ) varied significantly between the cutting scenarios as illustrated by Fig. 5 and the results of the adjusted model (Table 4). In agreement with our first hypothesis ( $H_1$ ), the cutting types ordered by decreasing  $\Delta PACL$  response were: gap creation, cutting from below, species-specific cutting, uniform cutting and cutting from above. This hypothesis was verified by ordering the slopes of the relationship ( $b_i$ ) between changes in PACL and cutting density for all the scenarios. The slope of this relationship was statistically different among cutting treatments except between cutting from below and species-specific cutting.

We found no evidence that the relationship between  $\Delta PACL$ , cutting type and cutting intensity depended on the initial stand structure. All likelihood ratio tests indicated that adding any stand parameter  $P_j$  in the model (Eq. (3)) did not significantly improve it.

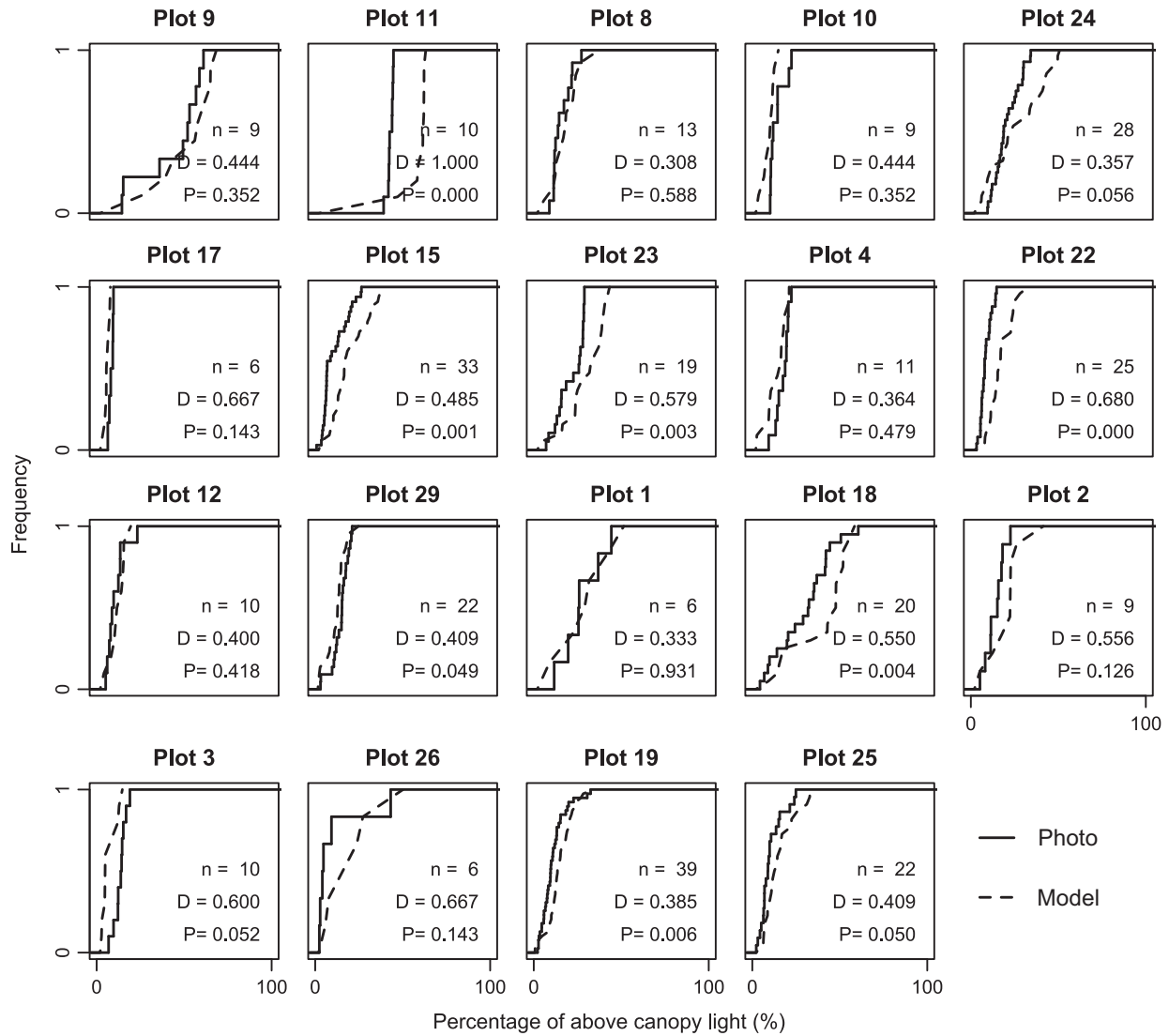


**Fig. 4.** Cumulative distribution function of modeled (dashed line) and measured (solid line) percentage of above canopy light (PACL). The number of measures and predicted PACL values ( $n$ ), the K-S test statistics ( $D$ ) and the associated  $P$ -value ( $P$ ) are also reported for each plot. The plots were ordered by decreasing oak proportion, as in Fig. 1.

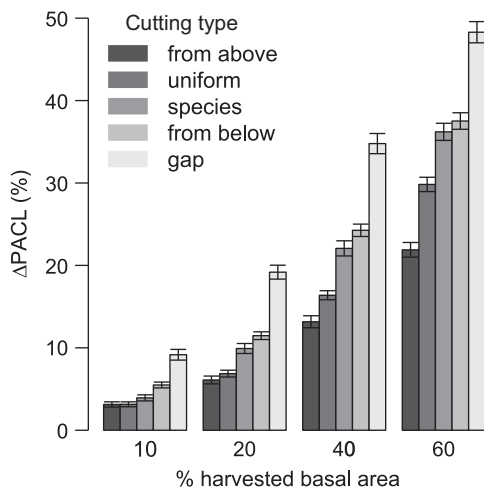


**Fig. 5.** Mean increase of transmitted light levels ( $\Delta$ PACL) by cutting scenario and by intensity. The adjusted mixed model indicated that the differences between cutting types are significant (Table 4) and accentuated as cutting intensity increased. Gap creation induced the greatest  $\Delta$ PACL responses.

**Table 4**

Fixed-effect estimates,  $b_i$ , of the adjusted model (Eq. (1)) with approximate confidence intervals with  $\alpha = 0.05$  (CI) and standard errors. Our model assumed that any removal of 1% of stand basal area induced an increase in PACL of  $b_i$ , additionally,  $\theta_\beta$  is the standard deviation of the random effect and indicated the variability of this relationship between plots.

Cutting type	$b_i$		$\theta_\beta$
	Estimates	CI	
Gap creation	0.835	0.76; 0.90	1.580
Cutting from below	0.615	0.57; 0.67	2.635
Species-specific cutting	0.579	0.53; 0.63	3.148
Uniform cutting	0.459	0.43; 0.48	3.870
Cutting from above	0.349	0.30; 0.40	0.172

Within the conditions of our sampled study sites, our first hypothesis appeared rather general and independent of initial stand conditions. Furthermore, the between-site variability of  $\Delta$ PACL response ( $\theta_\beta$  ranged from 0.172 to 3.870) was limited in comparison to the within-site variability ( $\theta_\epsilon = 4.150$ ).  $\Delta$ PACL response depended more likely on the conditions of the immediate surroundings of the measurement point rather than on general stand structure.

For the 9 plots where initial mean PACL was below 20% (Fig. 1), we analyzed the percentage of understorey area receiving PACL ranging between 0–10, 10–20, 20–40 or 40–100. Contrary to  $\Delta$ PACL, changes in percentage of microsites above a given light level depended noticeably on an interaction between cutting type and harvest intensity (Fig. 6) or post-harvest basal area (Fig. 7).

As most plots received an average of more than 10 PACL before harvest, the proportion of understorey area receiving less than 10 PACL decreased with harvest intensity (Fig. 6a). The proportion of microsites receiving 10–20 PACL also decreased rapidly with harvest intensity. Nevertheless, harvesting only 10% of stand basal area did not significantly reduce the proportion of these microsites except with gap creation (Fig. 6b). A cutting intensity of 10%, with all cutting types but gap creation, maintained basal area around 15–20 m<sup>2</sup> ha<sup>-1</sup> (Fig. 7b).

The different cutting scenarios provided very different proportions of microsites receiving 20–40 PACL which is the range of light conditions that promotes the less shade-tolerant oak (Figs. 6c and 7c). Gap creation maximized this proportion at 10% harvest intensity (target basal area 20–25 m<sup>2</sup> ha<sup>-1</sup>) but, at higher harvest intensities, very little area was in the 20–40 PACL range. Cutting from below and species-specific harvesting maximized the proportion of microsite receiving 20–40 PACL at about 20% of harvest intensity (target basal area of 15–20 m<sup>2</sup> ha<sup>-1</sup>) but they provided more than 40% of the area in the 20–40 PACL range in all but the most intense harvesting scenario. Uniform cutting maximized the area receiving 20–40 PACL at about 40% of harvest intensity (target basal area of 10–15 m<sup>2</sup> ha<sup>-1</sup>) whereas cutting from above provided about 40% of the area in the 20–40 PACL range independently of harvest intensity.

Cutting from above maintained a remarkably high proportion of microsites with less than 20 PACL at all cutting intensities and only created a low proportion of microsites with more than 40 PACL

(Fig. 6d). In contrast, the proportion of microsites with more than 40 PACL was the greatest for all cutting intensities with gap creation. The difference in microsite with greater than 40 PACL between gap-harvesting and the other cutting types was particularly notable at harvest intensity of 20%.

## 4. Discussion

### 4.1. Model parameterization and evaluation

Our relative simple light model used a mechanistic approach and provided satisfactory validation results. Compared to other forest radiative models (Cescatti, 1997; Brunner, 1998; Courbaud et al., 2003; Gersonde et al., 2004; Ligot et al., 2014), we utilized a model with a low number of input parameters and it was not necessary to calibrate by model inversion. Additionally, we performed a simulation of a large number of plots with diversified stand structures and compositions ranging from early-successional oak stands to late-successional beech stands. Stand density and initial light conditions were also very diverse and represented well the conditions in which oak regeneration might be desired. We therefore have confidence in our model's robustness for predicting understorey light in stands with varying stand structure and composition.

Overall, our model captured relatively well the variability of PACL independently of stand structure. The agreement between PACL<sub>photo</sub> and PACL<sub>model</sub> was satisfactory and in the range of previously reported studies (Law et al., 2001; Boivin et al., 2011). For some plots, PACL<sub>model</sub> slightly overestimated PACL<sub>photo</sub>. Such over-estimations mostly occurred in the presence of dense understorey trees (Beaudet et al., 2011) because some poles and trees had a dbh smaller than our inventory dbh threshold and because the

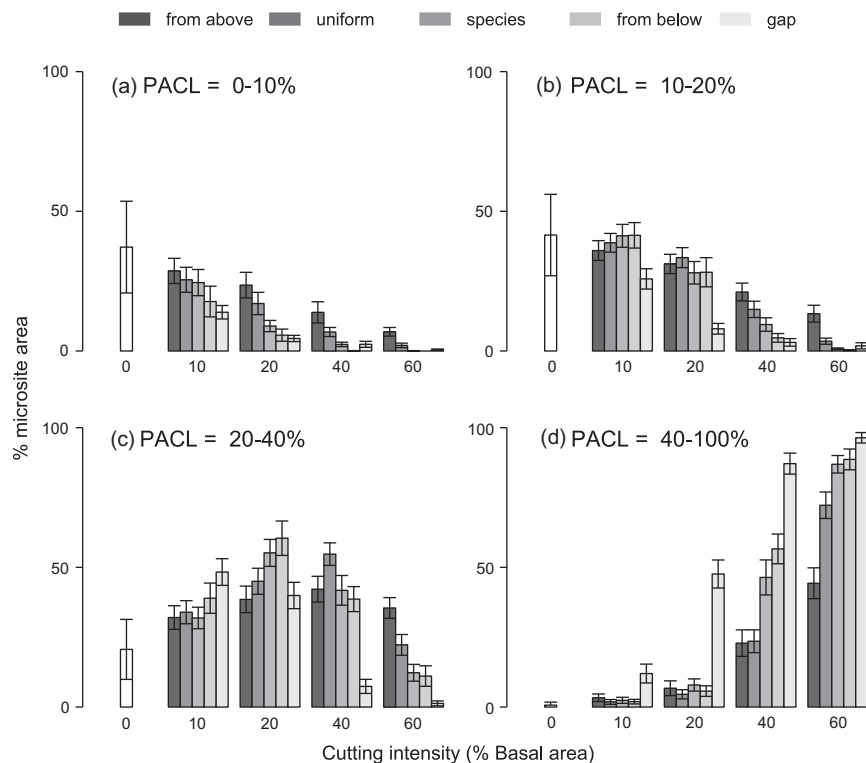


**Fig. 6.** Frequency of microsites with percentage of above canopy light (PACL) ranging between 0–10%, 10–20%, 20–40% and 40–100%. These frequencies were computed by harvest intensity in the 9 plots where initial mean PACL was below 20%. The proportion of microsites with PACL of 0–10 PACL (a) or 10–20 (b) was high prior to cutting (white bar on the left). This proportion decreased the most rapidly with gap creation in contrast with cutting from above. High proportions of microsites receiving 20–40 PACL (c) were obtained with 10% gap creation, 20% cutting from below, 20% species-specific cutting, or 40% uniform cutting.

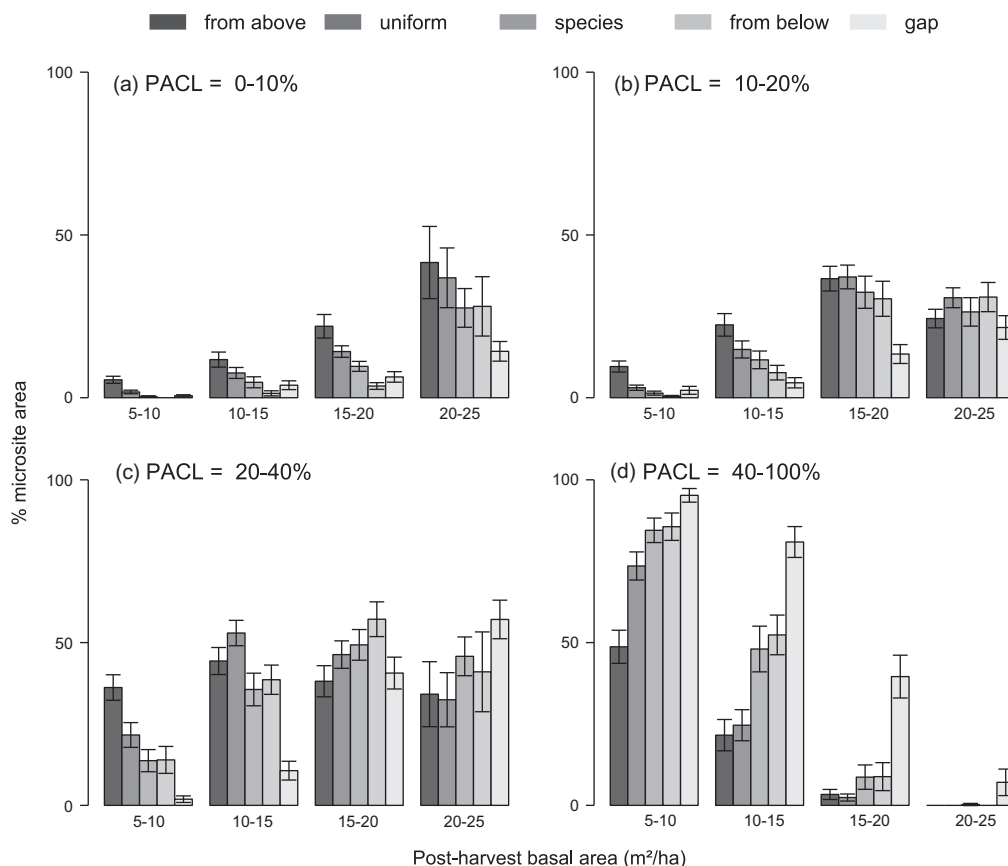


**Fig. 7.** Frequency of microsites by class of percentage of above canopy light (PACL) and post-harvest basal area. The frequencies were computed from the 9 plots where initial mean PACL was below 20% and, next, averaged by classes of post-harvest basal area. Cutting scenarios that maximized the understory area receiving 10–20 PACL (b) reduced stand basal area to about 15–20 m<sup>2</sup> ha<sup>-1</sup>. Cutting From above only slightly affected the proportion of microsites with 20–40 PACL (c). A High proportion of microsites with 20–40 PACL were obtained with cutting that created gaps that reduced basal area to 20–25 m<sup>2</sup> ha<sup>-1</sup>, with cutting from below that reduced basal area to 15–20 m<sup>2</sup> ha<sup>-1</sup>, or with uniform cutting and cutting from above that reduced basal area to 10–15 m<sup>2</sup> ha<sup>-1</sup>.

precision of PACL<sub>photo</sub> estimates was poorer in the presence of such dense understories. Nevertheless, the bias was of limited magnitude and, in this study, we did not focus on the absolute values of model predictions but instead analyzed how different cutting treatments affected both PACL average and distribution. However, these observations suggest that foresters should consider the density of understory trees before implementing different treatments to improve understory light conditions.

#### 4.2. Mean light response to the different cutting scenarios

The different cutting types led to different increases in mean PACL that were ordered according to our first hypothesis (H<sub>1</sub>) independently of initial stand structure and composition (in contradiction with H<sub>2</sub>). On average, harvesting 10% of stand basal area increased mean PACL by about 8.4% with gap creation, 6.2% with cutting from below, 5.8% with species-specific cutting, 4.6% with uniform cutting and 3.5% with cutting from above (Table 4 and Fig. 5).

Similar to the findings of numerous studies (Canham et al., 1994; Cescatti, 1997; Brunner, 1998; Stadt and Lieffers, 2000; Beaudet and Messier, 2002; Beaudet et al., 2011; Da Silva et al., 2012), the main factor limiting understory light was the absence of gaps between crowns. Consequently, at similar cutting intensities, harvests that create gaps strongly increased understory light. Additionally, we only considered immediate post-harvest conditions while the evolution of understory light several years after cutting may lead to increased or reduced differences between treatments. However, the increase in understory light due to the

creation of large gaps would be expected to last longer than the effects of the other cutting types since larger openings would take longer to close (Sprugel et al., 2009).

Another factor that strongly limits light availability for regeneration is the presence of a sub-layer of shade-tolerant species. We already noticed the influence of a dense understory when evaluating the performance of our light model. In addition, our simulation confirmed that understory trees might intercept a large proportion of light and that cutting from below can increase significantly understory light levels and can therefore be essential to promote the regeneration of less shade-tolerant species.

Preferentially harvesting shade-tolerant species, i.e. species-specific cutting, increased more transmitted light than harvesting trees randomly. Trees of shade-tolerant species intercept more light than trees of less shade-tolerant species since they have deeper, denser and wider crowns (Tables 2 and 3). Additionally, shade-tolerant species are usually more abundant in the understory than less shade-tolerant species. Species-specific cutting therefore tend to harvest a high proportion of poles and small trees similarly to the cutting from below.

##### 4.2.1. Optimum cutting scenario

The optimum cutting scenario within the context of this study maximized the understory area that is favorable to the natural regeneration of less shade-tolerant species, i.e. the area receiving 20–40 PACL. Contrary to mean PACL, the area receiving 20–40 PACL depended on the interactions between cutting type and cutting intensity. High proportions of microsites with 20–40 PACL were

obtained by either harvesting few trees or by harvesting more than 50% of stand basal area.

Creating gaps appears particularly promising to promote small clumps of oak regeneration with limited reduction of stand stocking. Gap harvesting the few trees located within and around these clumps largely increase the proportion of microsites with 20–40 PACL. In our simulations, the gaps that maximize this proportion of microsites are about 470 m<sup>2</sup> in size which corroborates the recommendations by von Lüpke (1998), Bruciamacchie and de Turckheim (2005) as well as the observation of Rugani et al. (2013) in old growth beech forests. These authors reported that oak regeneration was possible in gaps of at least 500 m<sup>2</sup> created by harvesting 4–5 mature trees (Bruciamacchie and de Turckheim, 2005). Larger gaps increase the proportion of microsites with more than 40 PACL and should likely be avoided during the first stages of regeneration development because such conditions are favorable to the rapid development of competitive herbaceous species (Gaudio et al., 2008; 2011).

Cutting from below and cutting preferentially shade-tolerant species were the best techniques to promote the recruitment of less shade-tolerant regeneration especially if saplings were uniformly spread in the understory as it happens after generalized masting. For the studied stands, the optimum harvest intensity was about 20% which corresponded approximately to a target basal area of about 15–20 m<sup>2</sup> ha<sup>-1</sup>.

Randomly cutting trees requires a greater harvest intensity to maximize the proportion of microsites with 20–40 PACL than gap creation, cutting from below and species-specific cutting. We obtained an optimum number of microsites with 20–40 PACL with a harvest intensity of 40% which corresponds to a target basal area of about 10–15 m<sup>2</sup> ha<sup>-1</sup> and agrees with the results obtained by Balandier et al. (2006) in even-aged oak stands.

Cutting from above generated the smallest increase in understory areas receiving less than 40% full light. It maintained a more asymmetric right-skewed distribution of PACL (Beaudet et al., 2011) than the other cuttings and hence a high proportion of microsites in shady conditions even after harvesting up to 60% of stand basal area. By preferentially eliminating large overstory oaks and maintaining low light levels in the understory, this treatment can be expected to quickly lead to a successional transition to dominance by shade-tolerant species.

In conclusion, promoting less shade-tolerant species can be achieved with various regeneration treatments. Forest managers

should consider whether the seedlings of less shade-tolerant species are aggregated or uniformly spread, whether a small reduction in stand stocking is more appropriate, and what is the desired composition of the different tree layers after harvest. The results from this study provide foresters with the necessary tools to evaluate how silvicultural treatments can be manipulated to create or maintain favorable conditions for the regeneration of species of different shade tolerance.

## Acknowledgements

This study was partly funded by the Walloon Region (Accord-Cadre de recherche et de vulgarisation forestières) and by the FNRS (Research Fellow grant awarded to G. Ligot). We are very grateful Benoît Mackels (ULg, Gembloux Agro-Bio Tech) and André Marquier (INRA, U.M.R. PIAF) for their help with the light measurements as well as to François de Coligny (INRA, AMAP) for his help programming our models in Capsis.

## Appendix A. Crown shape

Crowns were modeled with asymmetric ellipsoids.

$$\frac{(x - x_0)^2}{a} + \frac{(y - y_0)^2}{b} + \frac{(z + z_0)^2}{c} = 1 \quad (\text{A1})$$

$$a = (CR_{east} + CR_{west})/2$$

$$b = (CR_{north} + CR_{south})/2$$

$$c = (H - HCB)/2$$

With  $(x_0, y_0, z_0)$  the coordinates of the ellipsoid center and  $CR_{east}$ ,  $CR_{west}$ ,  $CR_{north}$ ,  $CR_{south}$  the crown radius measured toward the four cardinal directions,  $H$  the tree height and  $HCB$  to the base of the tree crown.

## Appendix B. Estimated distance between tree and photographer

The distance between the photographer and the tree trunk was not recorded in the field and, hence, estimated by considering that the photographer was 1.7 m tall and always aimed at the mid-height of the targeted crown:

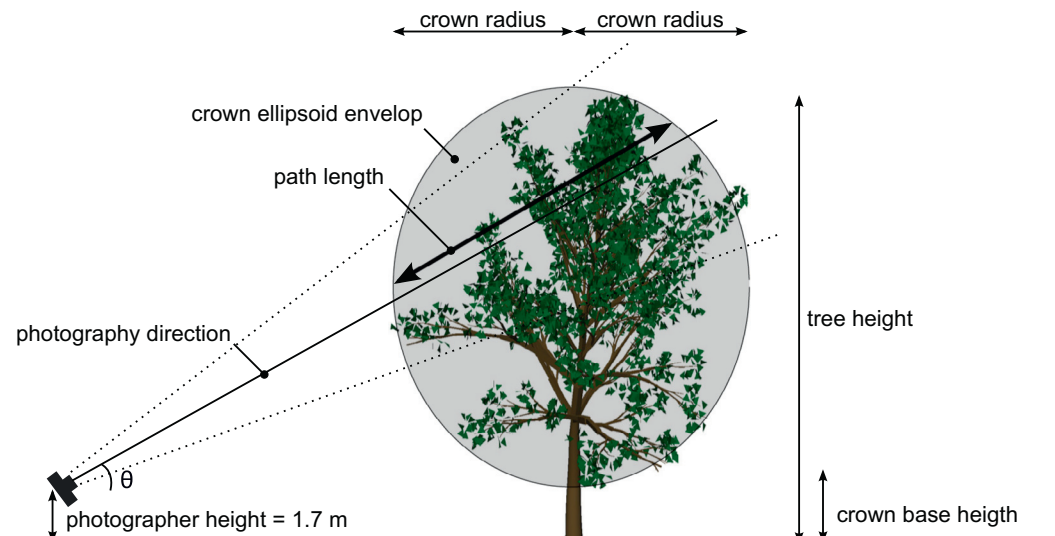


Fig. A1. Illustration of the different measurements involved in the computation of crown LAD.

**Table A1**

Stand structure and composition in the studied sites. The presented parameters are density (N), basal area (BA), quadratic mean diameter (Dg), the Clark–Evans aggregation index (CE) and the minimum (dbh<sub>min</sub>) and maximum (dbh<sub>max</sub>) of tree diameter. Plots are ordered by increasing oak proportion.

Plot	Stand				Oak				Beech			
	N (ha <sup>-1</sup> )	BA (m <sup>2</sup> ha <sup>-1</sup> )	Dg (cm)	CE	BA (m <sup>2</sup> ha <sup>-1</sup> )	Dg (cm)	dbh <sub>min</sub> (cm)	dbh <sub>max</sub> (cm)	BA (m <sup>2</sup> ha <sup>-1</sup> )	Dg (cm)	dbh <sub>min</sub> (cm)	dbh <sub>max</sub> (cm)
19	98	14.9	44.0	0.96					14.9	44.0	12.7	84.4
25	127	21.8	46.8	1.05					21.8	46.8	13.1	84.4
27	35	7.8	53.1	1.05					6.5	53.0	12.7	72.6
28	51	7.5	43.0	1.19	0.3	47.4	41.7	52.5	7.2	42.9	12.7	64.9
26	62	14.6	54.9	1.27	1.9	75.8	75.8	75.8	12.6	53.6	14.3	78.3
3	114	18.1	45.0	1.07	3.2	39.4	28.0	60.2	14.9	46.6	14.3	65.6
18	47	7.5	45.3	0.97	1.4	62.3	54.4	64.3	6.1	45.3	12.7	79.9
1	87	11.2	40.3	1.18	2.9	44.3	27.1	65.3	7.9	39.4	12.7	71.6
2	114	16.3	42.7	0.97	4.4	49.3	16.2	59.2	12.0	41.4	12.7	72.3
14	125	21.2	46.6	1.28	6.7	65.6	54.4	82.8	14.5	42.0	12.7	69.7
20	144	19.5	41.5	1.04	7.0	71.9	55.7	92.3	12.5	35.5	12.7	80.5
29	127	20.6	45.4	1.20	11.1	55.4	40.4	68.1	9.4	38.5	12.7	65.3
13	134	15.4	38.3	1.09	8.7	60.2	46.2	72.9	6.7	28.7	12.7	69.7
5	218	20.5	34.6	1.03	12.0	53.9	17.8	71.3	8.6	25.7	12.7	68.1
12	157	22.7	42.9	1.16	13.6	53.2	39.5	80.9	9.0	34.7	12.7	75.8
4	207	24.2	38.5	0.97	16.7	57.7	38.2	72.3	7.5	25.7	12.7	84.0
22	217	15.3	30.0	1.12	11.1	29.0	13.7	49.7	3.6	43.4	17.5	78.0
21	120	19.5	45.5	0.97	14.7	73.1	57.6	94.9	3.9	31.5	12.7	76.4
23	122	16.3	41.4	1.00	12.4	43.9	14.6	75.8	2.8	45.3	14.3	77.0
15	191	24.7	40.6	1.06	19.8	57.2	32.2	71.6	0.1	13.1	12.7	13.4
17	189	26.9	42.6	1.31	22.3	54.9	24.5	73.9	1.8	29.1	12.7	49.3
6	108	20.8	49.6	1.12	17.4	66.6	29.0	89.8	2.5	27.7	12.7	49.0
10	135	21.7	45.2	1.29	19.3	49.0	16.6	59.5	1.1	30.4	29.6	31.2
8	215	19.1	33.6	1.08	17.3	40.8	16.6	63.0	0.2	21.4	13.1	30.6
24	112	11.8	36.6	1.30	10.9	40.4	20.1	55.1				
11	115	14.4	40.1	1.00	13.5	48.2	12.7	66.9	0.2	19.7	17.5	21.7
9	123	12.7	36.4	1.25	12.5	37.5	13.2	69.7				

$$d = \frac{0.5(H - HBC) + HBC - 1.7}{\tan(\theta)} \quad (\text{A2})$$

With  $H$  tree height,  $HBC$  height to the base of the crown and  $\theta$  the recorded elevation angle (Fig. A1).

### Appendix C. Photograph direction

The equation of a photograph direction in a polar system in which the origin corresponding to the camera position is

$$x = L \cos(\theta) \cos(\alpha) \quad (\text{A3})$$

$$y = L \cos(\theta) \sin(\alpha)$$

$$z = L \sin(\theta)$$

with  $L$  the distance along the direction from the camera position,  $\theta$  the direction elevation angle and  $\alpha$  its azimuthal angle (Fig. A1).

### Appendix D. Path length computation

Computing the intersections between an ellipsoid and a line requires solving a second degree equation that can be expressed as:

$$AL^2 + BL + C = 0 \quad (\text{A4})$$

with,

$$A = \cos^2(\theta) \cos^2(\alpha)/a^2 + \cos^2(\theta) \sin^2(\alpha)/b^2 + \sin^2(\theta)/c^2$$

$$B = -2x_1 \cos(\theta) \cos(\alpha)/a^2 - 2y_1 \cos(\theta) \sin(\alpha)/b^2 - 2z_1 \sin(\theta)/c^2$$

$$C = x_1^2/a^2 + y_1^2/b^2 + z_1^2/c^2 - 1;$$

with  $(x_1, y_1, z_1)$  the coordinates of the ellipsoid center in the same coordinate system as the photograph direction. The distance between the intersected, i.e. the path length within the crown, is next given by the difference between  $L$  solutions.

Table A1

### References

- Adam, B., Benoit, J., Sinoquet, H., Balandier, P., Marquier, A., 2006. PiafPhotem - software to threshold hemispherical photographs. Version 1.0. In: UMR PIAF INRA-UBP, Clermont-Ferrand.
- Alderweireld, M., Ligot, G., Latte, N., Claessens, H., 2010. Le chêne en forêt ardennaise, un atout à préserver. Forêt Wallonne 109, 10–24.
- Astrup, R., Larson, B.C., 2006. Regional variability of species-specific crown openness for aspen and spruce in western boreal Canada. For. Ecol. Manage. 228, 241–250.
- Balandier, P., Sonohat, G., Sinoquet, H., Varlet-Grancher, C., Dumas, Y., 2006. Characterisation, prediction and relationships between different wavebands of solar radiation transmitted in the understorey of even-aged oak (*Quercus petraea*, *Q-robur*) stands. Trees 20, 363–370.
- Bartelink, H.H., 1997. Allometric relationships for biomass and leaf area of beech (*Fagus sylvatica* L.). Ann. For. Sci. 54, 39–50.
- Bates, D., Maechler, M., Bolker, B., Walker, S., 2013. lme4: Linear mixed-effects models using Eigen and S4.
- Beaudet, M., Brisson, J., Gravel, D., Messier, C., 2007. Effect of a major canopy disturbance on the coexistence of *Acer saccharum* and *Fagus grandifolia* in the understorey of an old-growth forest. J. Ecol. 95, 458–467.
- Beaudet, M., Harvey, B.D., Messier, C., Coates, K.D., Poulin, J., Kneeshaw, D.D., Brais, S., Bergeron, Y., 2011. Managing understorey light conditions in boreal mixedwoods through variation in the intensity and spatial pattern of harvest: a modelling approach. For. Ecol. Manage. 261, 84–94.
- Beaudet, M., Messier, C., 2002. Variation in canopy openness and light transmission following selection cutting in northern hardwood stands: an assessment based on hemispherical photographs. Agric. For. Meteorol. 110, 217–228.
- Boivin, F., Paquette, A., Racine, P.B., Messier, C., 2011. A fast and reliable method for the delineation of tree crown outlines for the computation of crown openness values and other crown parameters. Can. J. For. Res. 41, 1827–1835.
- Bruciamacchie, M., de Turckheim, B., 2005. La futaie irrégulière : théorie et pratique de la sylviculture irrégulière, continue et proche de la nature. Aix-en-Provence.
- Brunner, A., 1998. A light model for spatially explicit forest stand models. For. Ecol. Manage. 107, 19–46.
- Canham, C.D., Coates, K.D., Bartemucci, P., Quaglia, S., 1999. Measurement and modeling of spatially explicit variation in light transmission through interior cedar-hemlock forests of British Columbia. Can. J. For. Res. 29, 1775–1783.
- Canham, C.D., Finzi, A.C., Pacala, S.W., Burbank, D.H., 1994. Causes and consequences of resource heterogeneity in forests – interspecific variation in light transmission by canopy trees. Can. J. For. Res. 24, 337–349.
- Cescatti, A., 1997. Modelling the radiative transfer in discontinuous canopies of asymmetric crowns. I. Model structure and algorithms. Ecol. Model. 101, 263–274.
- Coates, K.D., Canham, C.D., Beaudet, M., Sachs, D.L., Messier, C., 2003. Use of a spatially explicit individual-tree model (SORTIE/BC) to explore the implications of patchiness in structurally complex forests. For. Ecol. Manage. 186, 297–310.

- Courbaud, B., de Coligny, F., Cordonnier, T., 2003. Simulating radiation distribution in a heterogeneous Norway spruce forest on a slope. *Agric. For. Meteorol.* 116, 1–18.
- Courbaud, B., Goreaud, F., Dreyfus, P., Bonnet, F.R., 2001. Evaluating thinning strategies using a tree distance dependent growth model: some examples based on the CAPSIS software “uneven-aged spruce forests” module. *For. Ecol. Manage.* 145, 15–28.
- Da Silva, D., Balandier, P., Boudon, F., Marquier, A., Godin, C., 2012. Modeling of light transmission under heterogeneous forest canopy: an appraisal of the effect of the precision level of crown description. *Ann. For. Sci.* 69, 191–193.
- Dufour-Kowalski, S., Courbaud, B., Dreyfus, P., Meredieu, C., De Coligny, F., 2012. Capsis: an open software framework and community for forest growth modelling. *Ann. For. Sci.* 69, 221–233.
- Emborg, J., 1998. Understorey light conditions and regeneration with respect to the structural dynamics of a near-natural temperate deciduous forest in Denmark. *For. Ecol. Manage.* 106, 83–95.
- Gaudio, N., Balandier, P., Marquier, A., 2008. Light-dependent development of two competitive species (*Rubus idaeus*, *Cytisus scoparius*) colonizing gaps in temperate forest. *Ann. For. Sci.* 65, 104, 101–105.
- Gaudio, N., Balandier, P., Philippe, G., Dumas, Y., Jean, F., Ginisty, C., 2011. Light-mediated influence of three understorey species (*Calluna vulgaris*, *Pteridium aquilinum*, *Molinia caerulea*) on the growth of *Pinus sylvestris* seedlings. *Eur. J. For. Res.* 130, 77–89.
- Gersonde, R., Battles, J.J., O'Hara, K.L., 2004. Characterizing the light environment in Sierra Nevada mixed-conifer forests using a spatially explicit light model. *Can. J. For. Res.* 34, 1332–1342.
- Henin, J.M., Huart, O., Rondeux, J., 2003. Biogeographical observations on four scolytids (Coleoptera, Scolytidae) and one lymexylonid (Coleoptera, Lymexylonidae) in Wallonia (Southern Belgium). *Belg. J. Zool.* 133, 175–180.
- Jonard, M., Andre, F., Ponette, Q., 2006. Modeling leaf dispersal in mixed hardwood forests using a ballistic approach. *Ecology* 87, 2306–2318.
- Kunstler, G., Curt, T., Bouchaud, M., Lepart, J., 2005. Growth, mortality, and morphological response of European beech and downy oak along a light gradient in sub-Mediterranean forest. *Can. J. For. Res.* 35, 1657–1668.
- Lafond, V., Lagarrigues, G., Cordonnier, T., Courbaud, B., 2013. Uneven-aged management options to promote forest resilience for climate change adaptation: effects of group selection and harvesting intensity. *Ann. For. Sci.*, 1–14.
- Law, B.E., Cescatti, A., Baldocchi, D.D., 2001. Leaf area distribution and radiative transfer in open-canopy forests: implications for mass and energy exchange. *Tree Physiol.* 21, 777–787.
- Lieffers, V.J., Messier, C., Stadt, K.J., Gendron, F., Comeau, P.G., 1999. Predicting and managing light in the understorey of boreal forests. *Can. J. For. Res.* 29, 796–811.
- Ligot, G., Balandier, P., Courbaud, B., Claessens, H., 2014. Forest radiative transfer models: which approach for which application? *Can. J. For. Res.* 44, 385–397.
- Ligot, G., Balandier, P., Fayolle, A., Lejeune, P., Claessens, H., 2013. Height competition between *Quercus petraea* and *Fagus sylvatica* natural regeneration in mixed and uneven-aged stands. *For. Ecol. Manage.* 304, 391–398.
- Nock, C.A., Caspersen, J.P., Thomas, S.C., 2008. Large ontogenetic declines in intra-crown leaf area index in two temperate deciduous tree species. *Ecology* 89, 744–753.
- Nyland, R.D., 1996. *Silviculture: Concepts and Applications*. McGraw-Hill, New-York.
- Phattaralerphong, J., Sathornkich, J., Sinoquet, H., 2006. A photographic gap fraction method for estimating leaf area of isolated trees: assessment with 3D digitized plants. *Tree Physiol.* 26, 1123–1136.
- Piboule, A., 2001. Validation et analyse de sensibilité d'un modèle de transfert radiatif en vue de son application à la cartographie de l'éclairement en peuplement forestier. In: ENGREF-INRA, Laboratoire d'Etude des Ressources Forêt-Bois.
- Pommerening, A., Murphy, S., 2004. A review of the history, definitions and methods of continuous cover forestry with special attention to afforestation and restocking. *Forestry* 77, 27–44.
- Prévost, M., Pothier, D., 2003. Partial cuts in a trembling aspen conifer stand: effects on microenvironmental conditions and regeneration dynamics. *Can. J. For. Res.* 33, 1–15.
- R Core Team, 2013. *R: A Language and Environment for Statistical Computing*. In: R Foundation for Statistical Computing, Vienna, Austria.
- Rugani, T., Diaci, J., Hladnik, D., 2013. Gap dynamics and structure of two old-growth beech forest remnants in Slovenia. *PLoS one* 8, 1–13.
- Schütz, J.-P., Pukkala, T., Donoso, P., Gadow, K., 2012. Historical emergence and current application of CCF. In: Pukkala, T., Gadow, K. (Eds.), *Continuous Cover Forestry*. Springer, Netherlands, pp. 1–28.
- Schütz, J.P., 1999. Close-to-nature silviculture: is this concept compatible with species diversity? *Forestry* 72, 359–366.
- Shinozaki, K., Yoda, K., Hozumi, K., Kira, T., 1964. A quantitative analysis of plant form—the pipe model theory: I. Basic analyses. *Jpn. Ecol.* 14, 97–105.
- Sprugel, D.G., Rascher, K.G., Gersonde, R., Dovciak, M., Lutz, J.A., Halpern, C.B., 2009. Spatially explicit modeling of overstorey manipulations in young forests: effects on stand structure and light. *Ecol. Model.* 220, 3565–3575.
- Stadt, K.J., Lieffers, V.J., 2000. MIXLIGHT: a flexible light transmission model for mixed-species forest stands. *Agric. For. Meteorol.* 102, 235–252.
- Stancioiu, P.T., O'Hara, K.L., 2006. Regeneration growth in different light environments of mixed species, multiaged, mountainous forests of Romania. *Eur. J. For. Res.* 125, 151–162.
- Takahashi, K., Goto, A., 2012. Morphological and physiological responses of beech and oak seedlings to canopy conditions: why does beech dominate the understorey of unmanaged oak fuelwood stands? *Can. J. For. Res.* 42, 1623–1630.
- von Lüpke, B., 1998. Silvicultural methods of oak regeneration with special respect to shade tolerant mixed species. *For. Ecol. Manage.* 106, 19–26.
- Wagner, S., Collet, C., Madsen, P., Nakashizuka, T., Nyland, R.D., Sagheb-Talebi, K., 2010. Beech regeneration research: from ecological to silvicultural aspects. *For. Ecol. Manage.* 259, 2172–2182.